ISSN 1024-8560, Atmospheric and Oceanic Optics, 2015, Vol. 28, No. 4, pp. 318–327. © Pleiades Publishing, Ltd., 2015.
Original Russian Text © N.V. Dudorova, B.D. Belan, 2015, published in Optika Atmosfery i Okeana.

ATMOSPHERIC RADIATION, OPTICAL WEATHER, AND CLIMATE

Thermal Balance of the Underlying Surface in Tomsk during 2004–2005

N. V. Dudorova and B. D. Belan

V.E. Zuev Institute of Atmospheric Optics, Siberian Branch, Russian Academy of Sciences, pl. Akademika Zueva 1, Tomsk, 634055 Russia

e-mail: ninosh@mail.ru, bbd@iao.ru

Received January 13, 2015

Abstract—The thermal balance of Tomsk for the period of 2004–2005 is studied. Heat flux to the soil and anthropogenic heat flux are calculated. The energy contribution of phase transitions of water to the net thermal balance is estimated. It is shown that heat is mainly gained due to radiation components (75–100%) from March to September; and from December to February the main contributor is turbulent heat flux, accounting for from 40 to 85% of the net balance. During the autumn period, before formation of snow cover, an important role in the incoming part is played by the heat flux from the soil, acting to increase the turbulent heat flux to the atmosphere. During the warm period, the heat loss is partitioned between the turbulent heat flux and heat losses due to water evaporation (50/50%). Heat lost to the soil makes a relatively small (no more than 10% of the total losses) contribution. In spring, on the expenditure side, there are heat losses due to snow cover melting, which can reach 50% of the total loss, in separate months. Wintertime heat losses are dominated by radiation components.

Keywords: city, thermal balance, turbulent flux, anthropogenic flux, evaporation rate

DOI: 10.1134/S1024856015040077

INTRODUCTION

Studying the thermal balance of different underlying surface types is important both from fundamental and applied points of view. On one hand, this is dictated by the need to understand the physical processes in the "underlying-surface – atmosphere" system, especially under the conditions of global climate warming. On the other hand, possible environmental changes due to global warming require updated methods for estimating the thermal balance in construction industries, housing and communal services, transportation, etc. In this regard, study of urban thermal balance becomes especially urgent because many additional energy sources are located on urban territory, leading to formation of additional heat and moisture flux sources [1–5]. There is also a simultaneous formation of stable updrafts of heated air (formation of urban "heat island"), which directly influence the climatic processes. Moreover, the additional moisture flux alters the absorbance of the surface atmosphere, thereby modifying the radiation balance of the underlying surface, playing a key part in the net radiation balance [6].

To study the thermal balance of the urban underlying surface, in addition to long-term coordinated measurements of many meteorological and physical characteristics, detailed information on urban economical activity is required to estimate the anthropogenic contribution. Also, to study the thermal balance of the urban underlying surface, it is important to select adequate methods for calculating some components of the thermal balance in accordance with available measurement conditions.

In this paper, in the framework of the study of the thermal balance in Tomsk, (a) the radiation balance is determined; (b) gradient techniques are used to calculate the turbulent heat and moisture fluxes, heat flux to soil, and anthropogenic heat flux; and (c) the energy contribution of phase transitions of water vapor to the net thermal balance is estimated.

The study was performed using data for Tomsk, available from: TOR station [7, 8]; AN-30 Optik-E airborne laboratory [9–11]; Tomsk Center for Hydrometeorology and Environmental Monitoring—branch of Federal State Budgetary Institution "Western Siberian Administration for Hydrometeorology and Environmental Monitoring" [12]; Observatory of Basic Experimental Complex (BEC) at Institute of Atmospheric Optics, Siberian Branch, Russian Academy of Sciences (BEC measurements are performed at heights of up to 40 m) [13, 14]; Federal State Statistics Service [15]; Open Joint-Stock Territorial Generating Company no. 11, Tomsk branch [16]; Tomsk Power Supply Open Joint-Stock Company [17]; Administration of State Inspection

Table 1. State of the underlying surface in the region of Tomsk during 2004 and 2005

Period of time	Underlying surface type	Date		ρ, g/cm^3	W, %	λ, W/(m °C)
		2004	2005			
1	Snow	Jan. 1–May 5 Nov. 11–Dec. 31	Jan. 1–Apr. 17 Nov. 3–Dec. 31	0.1–0.31	–	0.03–0.27
2	Frost soil without snow cover	– Oct. 17–Nov. 10	Apr. 18–30 –	– –	– –	1.00
3	Soil	May 6–Oct. 17	May 1–Nov. 3	1.3	7 (dry) 17 (wet, without puddles) 24 (wet, with puddles)	0.33 0.78 0.85

Here, ρ is the density of underlying surface; W is underlying surface wetness; and λ is the coefficient of the underlying surface.

for Road Traffic Safety, Administration of Ministry of Internal Affairs of Russia, Tomsk region [18].

1. METHOD FOR CALCULATING THE THERMAL BALANCE COMPONENTS

The thermal balance of the underlying surface is an expression of the energy conservation law in the case of interaction of solar, atmospheric, and terrestrial radiation. Taking into account human economic activity, the equation for thermal balance can be written as [1]:

$$R + Q_F = Q_S + Q_H + Q_E + Q_T, \quad (1)$$

where R is the radiation balance of the underlying surface; Q_F is the anthropogenic heat flux, Q_S is the heat flux between the underlying surface and underlying layers, Q_H is the turbulent heat flux between the underlying surface and the atmosphere, Q_E and Q_T are heat fluxes associated with water phase transformations, Q_E is the heat flux associated with evaporation and condensation, and Q_T is the heat flux associated with ice melting and water freezing.

The radiation balance of the underlying surface R is the most significant component of the thermal balance equation; it is defined as the difference between absorbed solar radiation and effective emission of the underlying surface. The calculation technique and detailed results of studying the urban radiation balance were discussed in work [19]. In the case when solar and downward radiations of the atmosphere exceed the outgoing radiation, R takes positive values. The anthropogenic heat flux Q_F is always positive in value. The calculation technique and detailed results of studying the anthropogenic heat flux were published in earlier work [20]. When the right-hand side of equation (1) is nonzero, heat fluxes to the atmosphere and soil may arise.

In accordance with formula (1), the turbulent heat flux Q_H is considered to be positive when the underlying surface releases heat to the atmosphere, i.e., when heat flux is directed upward; on the contrary, the heat flux is considered to be negative when the atmosphere heats the underlying surface, i.e., when heat flux is directed downward. Analogously, the heat flux Q_E, associated with evaporation and condensation, is positive in the case of evaporation from the underlying surface; on the contrary, the flux is negative if water vapor condenses onto the underlying surface. The heat flux between the underlying surface and underlying layers Q_S is positive when the lower soil layers are colder than the upper soil layers, i.e., when the heat flux is directed from the underlying surface to soil depth; and the heat flux will be negative in the opposite situation. The heat flux Q_T, associated with ice melting and water freezing, is positive when snow cover melts; and this flux is negative when water on the underlying surface freezes.

1.1. Heat Flux between Underlying Surface and Underlying Layers

The heat flux between the underlying surface and underlying layers is traditionally described by the Fourier law [6, 21]:

$$Q_S = -\lambda \frac{\partial t}{\partial z}, \quad (2)$$

where λ is the thermal conductivity coefficient of the underlying surface, and $\partial t/\partial z$ is the temperature gradient of the soil.

The thermal conductivity coefficient of the underlying surface depends essentially on surface type, density, and moisture content. The thermal conductivity coefficient of the underlying surface was determined by an indirect method because no direct regular measurements of soil thermodynamic characteristics were available. Table 1 presents characteristic underlying

surface types and certain surface parameters. Based on the data available from meteorological stations, each year was divided into three periods: Period 1 with snow cover present; Period 2 with negative soil surface temperature (without snow cover); and Period 3 with positive soil surface temperature (without snow cover).

For the Period 1, the heat flux was defined by the formula

$$Q_S = -\lambda_{sn}\frac{(t_0 - t_{sn})}{h_{sn}}, \quad (3)$$

where the thermal conductivity coefficient of snow λ_{sn} in units of W/(m °C) was calculated according to the Abels' formula, $\lambda_{sn} = 2.85\times10^{-6}\rho_{sn}^2$ [22] (ρ_{sn} is snow density in kg/m^3); t_{sn} is the temperature of snow surface, t_0 is the surface temperature of snow-covered soil; and h_{sn} is the height of snow cover.

For the periods 2 and 3, the heat flux was calculated from the formula

$$Q_S = -\lambda_s\frac{(t_{0.2} - t_0)}{0.2}, \quad (4)$$

where $\lambda_s = k_s C_v$ is the thermal conductivity coefficient of soil [23]; k_s is the temperature conductivity of soil in cm^2/s; C_v is the volume heat capacity of soil in cal/(cm^3 °C); and $t_{0.2}$ is the soil temperature at a depth of 0.2 m.

The thermal diffusivity and specific heat of soil were calculated using the following formulas, derived on the basis of the Gupallo method [2]:

$$k_s = (2.1^{1.4-0.02W}\rho_s^{0.8} \times \exp\left[-0.007(W-20)^2\right] + \rho_s^{0.8+0.02W})\times10^{-3}; \quad (5)$$

$$C_v = \rho_s\left(0.2 + \frac{W}{100}\right). \quad (6)$$

Here, ρ_s is the soil density in g/cm^3.

The error of this method for calculating the thermal-physics parameters does not exceed 7.4% [2]. Data for the study were provided by the Tomsk Center for Hydrometeorology and Environmental Monitoring—branch of the Federal State Budgetary Institution "Western Siberian Administration for Hydrometeorology and Environmental Monitoring". The soil density was taken as an average of densities typical for soils in Tomsk [22]. The soil moisture content was estimated on the basis of reference information on hydrological characteristics of a given type of soils [23] and data on the state of soil surface available from the meteorological station.

1.2. Turbulent Heat Flux

The turbulent heat flux Q_H is usually determined using two approaches: calculation on the basis of inertialess measurements of temperature and vertical wind velocity components [24], as well as on the basis of indirect methods, relying on measurements of averaged meteorological variables (gradient methods) [2–4]. The method for determining the turbulent heat and moisture fluxes is used in this paper; it is based on gradient measurements and is more preferable for long-term studies.

The approach of Taylor and Schmidt suggests that, when the process of turbulent mixing of air masses is considered analogously to molecular diffusion, the formula for the vertical turbulent heat flux in the surface air layer has the form [2]:

$$Q_H = -C_p\rho_a k\frac{\partial\Theta}{\partial z}, \quad (7)$$

where $C_p = 1006$ J/(kg K) is the specific heat of air at constant pressure; $\rho_a = \dfrac{P}{R_c T}$ is the air density, calculated on the basis of measurements of pressure P (hPa) and absolute air temperature T (K); $R_c = 287$ J/(kg K) is the specific gas constant of dry air; k is the turbulence coefficient; $\partial\Theta/\partial z$ is the vertical gradient of potential air temperature.

The turbulence coefficient was determined according to the formula in which the stability parameter of the atmosphere is represented by the Richardson number [3]:

$$k = \chi^2 z\frac{\Delta u}{\ln\dfrac{z_1}{z_2}}\left[1 - \frac{hg}{T}\frac{\Delta\Theta}{(\Delta u)^2}\frac{\left(\ln\dfrac{z_1}{z_2}\right)^2}{\ln\left(\dfrac{z_3}{z_4}\right)}\right]. \quad (8)$$

Here, $\chi = 0.38$ is the dimensionless von Kármán constant; z is the height between z_1 and z_4, for which k is calculated; $\Delta u = u_1 - u_2$ is the difference between wind speeds at heights z_1 and z_2; $\Delta\Theta = \Theta_3 - \Theta_4$ is the difference between potential temperatures at heights z_3 and z_4; h is the height of the surface layer (assumed to be 30 m); and g is the acceleration due to gravity.

Usually, the meteorological parameters (the air temperature and humidity and wind speed) in the surface air layer vary with height proportionally to the logarithm of height [25]. Then, the gradient of the potential temperature of air can be expressed as follows:

$$\frac{\partial\Theta}{\partial z} = \frac{1}{z}\frac{(\Theta_1 - \Theta_2)}{\ln(z_1/z_2)}, \quad (9)$$

where Θ_1 and Θ_2 are potential temperatures at heights z_1 and z_2, respectively; z is a height between z_1 and z_2, at which the gradient of Θ is calculated.

The potential temperature was calculated from the standard formula

$$\Theta = T\left(\frac{10^5\ \text{Pa}}{P}\right)^{R_c/C_p}. \quad (10)$$

When pressure measurements at required heights were absent, we used the following formula:

$$P = P_0 \exp\left(-\frac{gz}{R_c T}\right), \quad (11)$$

where P_0 is the pressure near the underlying surface.

The air temperature and wind speed were measured at the BEC observatory [13, 14] with the purpose of determining turbulent heat flux (7). The turbulence coefficient and the gradient of potential temperature were calculated for the height of 20 m, which was within the surface air layer.

1.3. Heat Fluxes due to Phase Transitions of Water Vapor

Evaporation and condensation. Heat fluxes due to water evaporation and water vapor condensation are calculated from the formula [5, 6]:

$$Q_E = -L\rho_a k \frac{\partial s}{\partial z}, \quad (12)$$

where $L = 4.18 \times 10^3 (597.26 - 0.647t)$ is the specific heat of vaporization (evaporation) in J/kg; t is the air temperature in °C; $\partial s/\partial z$ is the vertical gradient of air specific humidity.

The specific humidity s (g/kg) was calculated using the standard formula [6]:

$$s = \frac{0.622e}{P - 0.378e} \times 10^3, \quad (13)$$

where

$$e = \frac{ERh}{100\%} \quad (14)$$

is the partial pressure of water vapor in hPa; Rh is the relative air humidity in %;

$$E = 6.107 \times 10^{\frac{at}{b+t}} \quad (15)$$

is the water vapor saturation pressure in hPa; and a and b are the coefficients, which depend on air temperature (if $t > 0$, then $a = 7.633$, $b = 241.9$; if $t < -40$, then $a = 9.5$, $b = 265.5$; and if $40 < t < 0$, then $a = -0.0475t + 7.63$, $b = -0.62t + 241.9$).

By analogy to the turbulent heat flux, the heat flux due to water evaporation and water vapor condensation was calculated for the height of 20 m; and the air temperature and wind speed, measured at heights of 10 and 30 m were provided by the BEC observatory.

Melting and freezing. Water transition from solid to liquid phase on the Earth's surface, like the reverse process, is accompanied by either heat gain or loss. This component of thermal balance Q_T is important to take into account when monthly average totals of thermal balance at midlatitudes are calculated, especially in the spring period, during intense snow cover melting.

The heat fluxes due to snow melting Q_{T+} and due to freezing water bodies and water on the soil surface Q_{T-} were calculated using the following formulas [6]:

$$Q_{T+} = \rho_{sn} \Delta h_{sn} \lambda_w / \Delta t, \quad (17)$$

$$Q_{T-} = -\rho_w \Delta h_{pr} \lambda_w / \Delta t, \quad (18)$$

where $\rho_w = 998.2$ is the water density in kg/m^3; Δh_{sn} is change in the height of snow cover over Δt; Δh_{pr} is the amount of liquid precipitation, having frozen in time Δt; and $\lambda_w = 335 \times 10^3$ is the specific melting and crystallization heats of water in J/kg.

The upper bound estimate of Q_{T-} in the autumn period, as well as after thaw episodes in the spring and winter periods, was obtained by taking Δh_{pr} to be equal to the total amount of liquid precipitation a day before the underlying surface temperatures became negative; and the freezing time Δt was assumed to be equal to 6 h. Data for the study were provided by Tomsk Center for Hydrometeorology and Environmental Monitoring – branch of Federal State Budgetary Institution "Western Siberian Administration for Hydrometeorology and Environmental Monitoring".

Condensation of anthropogenic moisture. Some water vapor amount is known to be released to the atmosphere during fuel combustion. In the general form, the reaction of hydrocarbon combustion can be written as [26]:

$$C_m H_n + \left(m + \frac{n}{4}\right) O_2 = nCO_2 + \frac{n}{2} H_2O + \text{heat}, \quad (19)$$

where m and n are the numbers of carbon and hydrogen atoms in the molecule.

Table 2 presents the relative contents of different hydrocarbons in diverse fuel types (gasoline and natural and liquefied gas) [26], as well as the mean composition of other fuel types (diesel fuel, kerosene, etc.), obtained on the basis of reference literature (designated as conventional fuel in the table).

When the hydrocarbon fraction in fuel is known, formula (19) can be used to calculate the water amount released when one unit of fuel mass is burned (Table 3).

As a result, it is found that combustion of one unit of natural gas mass is accompanied by the release of 2.16 units of water vapor; liquefied gas, by 1.97 units; and gasoline, by 1.37 units. The released water amount was assumed to be 1.33 units of mass for the other fuel types.

The monthly average heat flux, formed due to condensation of anthropogenic water vapor, was determined according to the formula

$$Q_z = \frac{NL}{S\Delta t}, \quad (20)$$

Table 2. Percentage (by mass) of different hydrocarbons in the compositions of diverse fuel types

Hydrocarbon	Chemical formula	Conventional fuel, %	Gasoline, %	Natural gas, %	Liquefied gas, %
Methane	CH_4	–	–	94	–
Ethane	C_2H_6	–	–	2	–
Ethylene	C_2H_4	–	–	–	–
Acetylene	C_2H_2	–	–	–	–
Propane	C_3H_8	–	–	–	90
Propene	C_3H_6	–	–	2	–
Butane	C_4H_{10}	4	–	2	10
Pentane	C_5H_{12}	23	–	–	–
Hexane	C_6H_{14}	28	–	–	–
Heptane	C_7H_{16}	11	10	–	–
Toluene	$C_6H_5CH_3$	10	–	–	–
Octane	C_8H_{18}	12	–	–	–
Xylene	$C_6H_4(CH_3)_2$	8	–	–	–
Nonane	C_9H_{20}	2.5	–	–	–
Decane	$C_{10}H_{22}$	1.5	–	–	–
Isooctane	C_7H_{15}	–	90	–	–

Table 3. Mean molar mass of different fuel types and amount of water vapor, released due to combustion of a unit of fuel

Index	Conventional fuel	Gasoline	Natural gas	Liquefied gas
Mean molar mass	90.65	99.1	17.68	47.6
Water amount in a unit of conventional fuel	1.33	1.37	2.16	1.97

where N is the mass of water emitted to the urban atmosphere in the case of combustion of different fuel types in time Δt (over 1 month); and $S = 2.946 \times 10^8$ m^2 is the area of Tomsk.

Data for the study were provided by Territorial body of Federal State Statistics Service in Tomsk region (Tomskstat).

2. RESULTS AND DISCUSSION

2.1. Components of Thermal Balance

The study of the radiation balance in Tomsk [19] showed that the radiation balance R was positive for the most part of the year and negative in November, December, and January. The maximum was observed in June and was found to be 176 W/m^2 in 2004 and 167 W/m^2 in 2005, and minimum was observed in December and equaled –26 W/m^2 in 2004 and –41 W/m^2 in 2005, thus suggesting that the radiation influx is smaller than the emission of underlying surface and lower atmospheric layers in the cold period of the year.

Analysis of components of anthropogenic heat flux showed that fuel burning makes the largest contribution to the total flux Q_F [20]. The factor ranked second in significance is energy leaks from heated buildings. Electrical energy gives the smallest contribution to air heating. The anthropogenic heat influx is significant in winter months and is of the order of 16–18 W/m^2, comparable with total solar radiative flux (Fig. 1). In summer months, Q_F contributes insignificantly to the net thermal balance and is equal to 2–4 W/m^2.

Figure 2 shows the annual behavior of the monthly average heat flux to soil Q_S in Tomsk. For comparison, this figure also presents a similar flux for Lodz [27], i.e., the most closely lying city among those for which published results are available. We note that annual variations in the heat flux Q_S are very similar in Tomsk and Lodz; however, the wintertime Q_S values in Lodz are much lower than in Tomsk (comparable with autumn values in Tomsk). A stronger wintertime soil cooling in Lodz as compared to that in Tomsk can be explained by lower snow cover height.

The Q_S values substantially differ between April of 2004 and 2005 in Tomsk, primarily because the snow cover in spring of 2004 was removed quite late, i.e., in early May; while snow cover in spring of 2005 was removed in mid-April, which is characteristic for

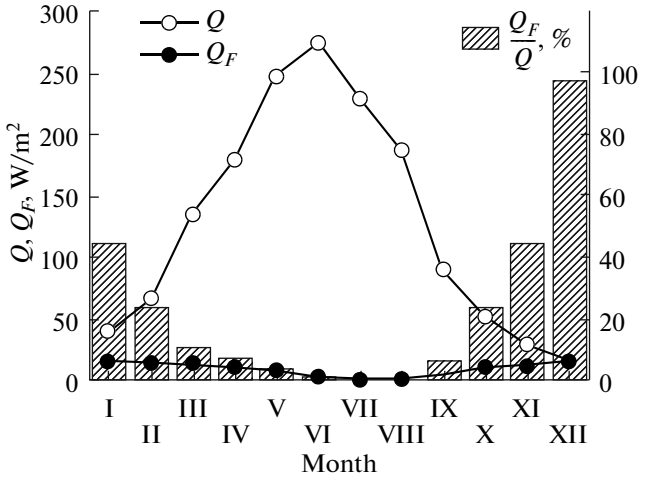

Fig. 1. Annual variations in the total solar radiation Q, anthropogenic urban heat flux Q_F, as well as their relationship in Tomsk during 2004.

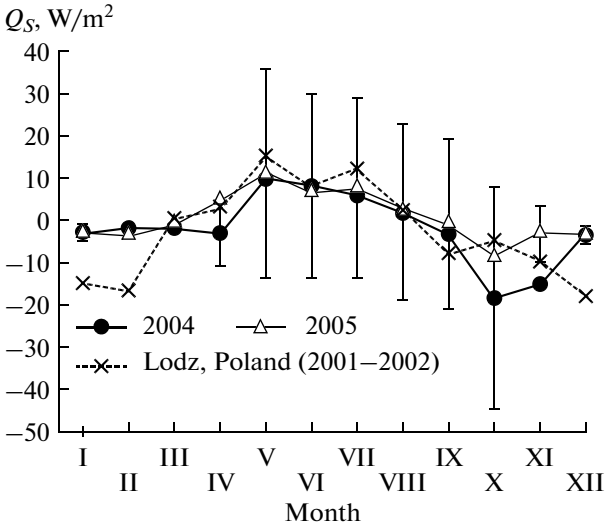

Fig. 2. Annual variations in the heat fluxes to soil in Tomsk and Lodz.

Tomsk (see Table 1). Seemingly, the diurnal behavior of Q_S in April, 2004, was similar to its behavior in winter months, when the temperature of the snow surface was below the temperature of the snow-covered soil. The soil surface temperature started to rise appreciably in April, 2005, after removal of the snow cover. Since deep soil layers had little time to warm, the daytime temperature gradient on the snow-free soil surface was substantial (up to 114 °C/m), and the peak values of heat flux exceeded 80 W/m^2. However, the high daytime Q_S values were balanced by negative nighttime values in view of the fact that nighttime frosts still remained and the soil temperature gradient was negative.

The maximal Q_S value in Tomsk falls within springtime period of soil heating after removal of snow cover. During summer, the Q_S value falls to zero because of the gradual heating of underlying soil layers. The maximal (in modulus) negative Q_S value, corresponding to upward heat flux from underlying layers, corresponds to the autumn period of frosts in the absence of stable snow cover. The wintertime monthly average Q_S values assume the largest (in modulus) negative values, primarily because of the presence of high snow cover, possessing good thermal insulating properties.

The Q_S values in October and November, 2004, were several-fold larger (in modulus) than the corresponding values in 2005, both due to a time lag in the formation of snow cover, and to different soil temperatures and moisture contents. The snow cover had formed on November 14 in 2004, much later than in 2005 (see Table 1). Correspondingly, thermal insulation properties of snow in 2005 strongly decreased the heat flux from the underlying soil layers. Moreover, snow had covered yet unfrozen soil in 2005; whereas in 2004 the soil surface temperature had been negative since October 17 (almost one month before formation of constant snow cover). The thermal conductivity coefficient is known to be much larger for ice than for water and air. Correspondingly, frozen wetted soil in October–November of 2004 had a larger thermal conductivity coefficient than nonfrozen soil in 2005, which added to the substantial difference in autumn values of heat flux.

Figure 3 shows the annual behavior of turbulent heat flux Q_H. It can be seen that the annual behavior of Q_H agrees well with the literature data (Lodz, Poland [27]), if we take into account the specific features of local climate. Similar to the radiation balance, maxima in Q_H are observed in June of both years, magnitudes being 76 W/m^2 in 2004 and 68 W/m^2 in 2005; and Q_H minima are observed in December and are equal to −21 W/m^2 (2004) and −45 W/m^2 (2005). We note that marked February differences in Q_H are explained by numerous temperature inversions in 2005, which were caused by an anticyclone with very low air temperatures that had been stable in that period of time.

In both years, the symmetric bell-shaped curves, characteristic for R, are markedly deformed in that monthly average Q_H value decreases more slowly in the autumn period. This can be readily explained by heat supply from overlying soil layers (due to soil cooling before snow cover formation), accompanied by turbulent heat transfer from the underlying surface to the atmosphere.

Figures 4 and 5 show the monthly average variations in Q_S and Q_H, respectively, in order to compare the diurnal variations in the components of thermal balance. It can be seen that strong nighttime soil cooling takes place in October (see Fig. 4). At the same time, the turbulent heat flux becomes positive in sign

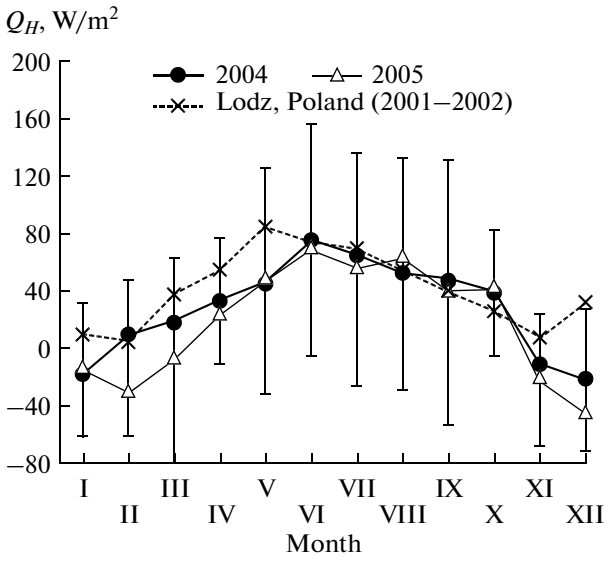

Fig. 3. Annual variations in the turbulent heat flux in Tomsk and Lodz.

(see Fig. 5), despite the negative nighttime Q_H values throughout the year, meaning that the heat flux is directed from the atmosphere to the underlying surface. The effect of enhancement of turbulent heat flux due to intense soil cooling was especially distinct in 2004, when snow cover had formed later than usual, and frosts began too early.

Figure 6 shows the annual behavior of the heat flux due to water evaporation and condensation, as well as heat losses due to snow cover melting. It can be seen that the maximum of monthly average value of the heat flux, associated with water evaporation and condensation, is 90–100 W/m^2 and corresponds to the warmest month of July, characterized by maximal specific humidity. The Q_E values are maximal in the cold period of the year.

Springtime heat losses due to snow cover melting are significant in the thermal balance of the urban underlying surface. In periods of intense snow melt, the maximal daily average value of Q_{T+} was 144 W/m^2 in 2004 and 112 W/m^2 in 2005. The average Q_{T+} values were 34.3 W/m^2 in April, 2004, and 19.8 W/m^2 in April, 2005, comparable to heat losses due to evaporation Q_E and accounting for 50 and 30% of the total heat loss, respectively. The difference in the total heat lost, due to snow melting, between 2004 and 2005 is explained by the difference in snow cover thickness.

Estimation of the heat flux, released due to the freezing of water bodies and water on soil surface during autumn, showed that peak Q_{T-} values at frost onset may reach a few tens of W/m^2. However, when autumn frosts occur at their normal frequency (from one to three times a month), the monthly average Q_{T-} value is about 1–2 W/m^2 in the net thermal balance. In addition, usually alternating frosts and thaws in the fall period are characterized by sign-alternating heat fluxes (negative fluxes due to water freezing and positive fluxes due to snow melt) and, correspondingly, cancel each other when monthly average Q_{T-} values are calculated. Thus, it can be concluded that the heat flux, released due to the freezing of water bodies and

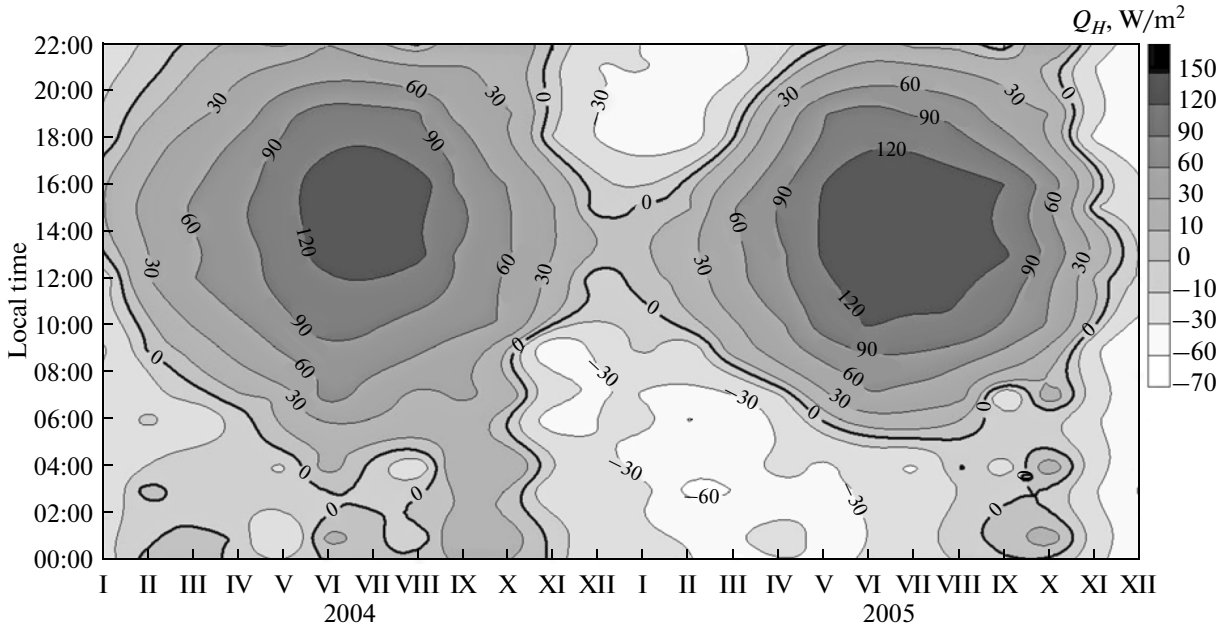

Fig. 4. Diurnal variations in the turbulent heat flux in Tomsk during different months of 2004–2005.

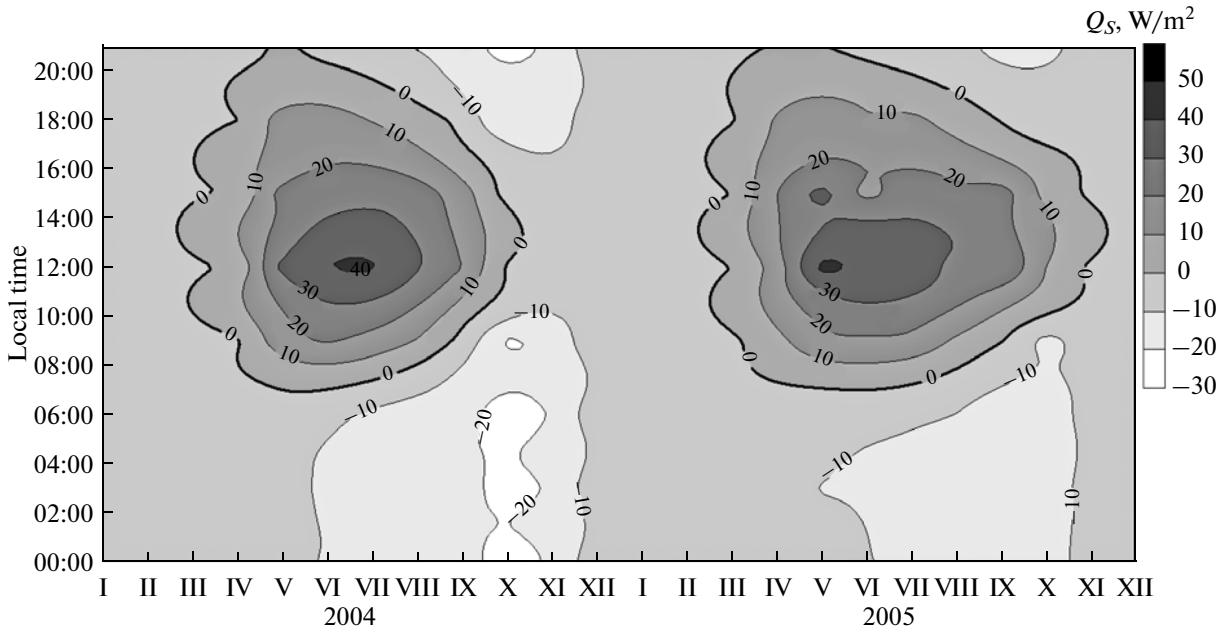

Fig. 5. Diurnal variations in the heat flux to soil in Tomsk in different months of 2004–2005.

water on the soil surface, is immaterial when the net heat balance of the underlying surface is determined.

The meteorological variables, required to calculate Q_E, were measured in the suburbs of the city [13, 14]; therefore, an additional heat gain due to condensation of moisture coming from anthropogenic urban sources, which is omitted in Q_F, should be estimated to determine the net thermal balance of the urban underlying surface Q_F. When the volume of burned fuel is known, we can determine the amount of moisture released during combustion. For instance, burning different fuel types injects 450–600 thousand tons of water to the atmosphere of Tomsk in the winter months and 70–300 thousand tons during summer. Assuming that all moisture emitted to the urban atmosphere due to fuel burning is condensed within city precincts, we can estimate the maximum monthly average heat flux, released due to condensation of anthropogenic water vapor; the flux was found to be 1.0–1.9 in winter and 0.2–1.0 W/m^2 in summer. It should be noted that we cannot determine exactly what part of moisture from anthropogenic sources was condensed within city precincts and what beyond. However, our upper bound estimate shows that this component is minor and, as such, can be neglected in the net thermal balance.

2.2. Net Thermal Balance

We will compare all above-mentioned components of thermal balance. Figure 7 shows annual variations in the components of the urban thermal balance for the two years considered here. For ease of comparison, the components in the right-hand side of equation (1) are shown in the figure with opposite sign. In this case, the flux directed to the underlying surface has positive values, while the flux directed outward from the underlying surface (heat is lost to the atmosphere or soil) has negative values.

It is found that most heat is gained due to radiation components R from March to September, with these components being the only suppliers of heat to the underlying surface. In the fall period, a major part of

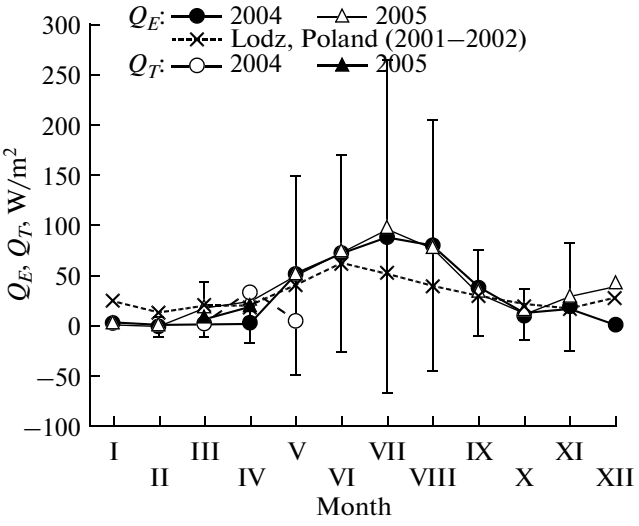

Fig. 6. Annual variations in the heat losses due to evaporation Q_E and due to snow cover melting Q_T during spring period of time in Tomsk and Lodz.

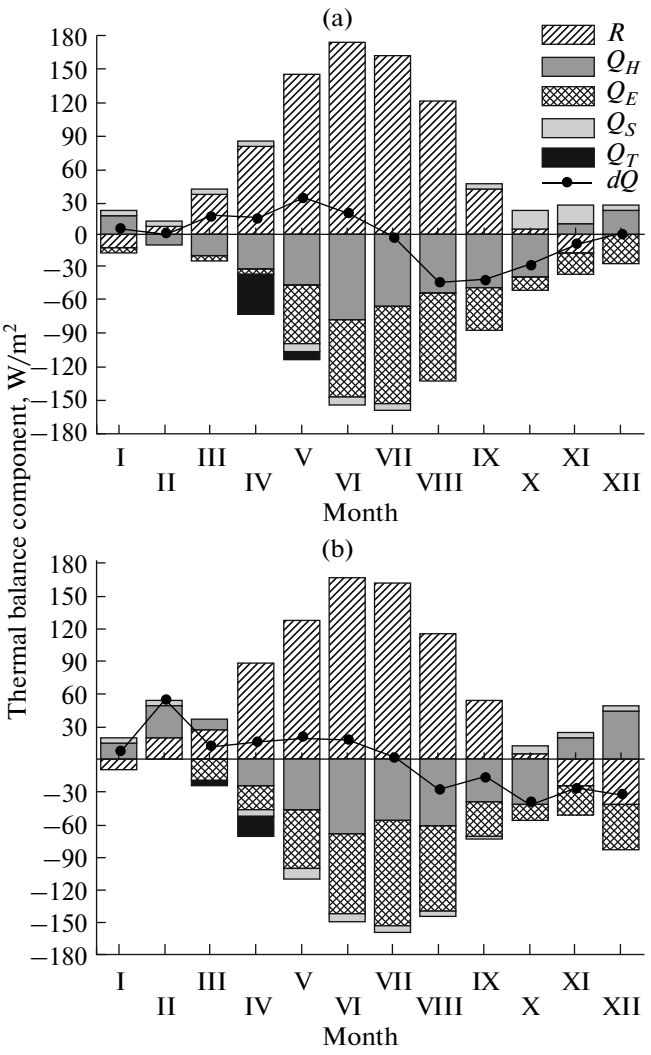

Fig. 7. Annual variations in the thermal balance components in Tomsk during (a) 2004 and (b) 2005.

the incoming part is played by the heat flux from the underlying layers of Earth Q_S, adding to the turbulent heat flux Q_H into the atmosphere in this period of time. From December to February, the heat mainly comes to the underlying surface from the atmosphere due to turbulent mixing in the presence of temperature inversions, and it accounts for from 40 to 85% of the total heat gain.

The heat losses in summer and fall are almost equally divided between turbulent heat flux Q_H and losses due to water evaporation Q_E. The heat lost to soil Q_S is characterized by relatively small values (no more than 10% of the total losses) during spring and summer. Most wintertime heat losses are associated with the radiation components R. In spring, a significant contribution to the expense part comes from heat losses due to snow cover melting Q_{T+}, which can reach 50% of the total losses in separate months.

The curve with symbols in Fig. 7 shows the difference between heat gain and loss at the underlying surface, dQ, which, in accordance with thermal balance equation (1), must be zero. It should be noted that the annual behavior of this heat difference correlates well with the annual behavior of the heat flux to the soil (see Fig. 2), showing a maximum in May and a minimum in October. It is noteworthy that, as was already indicated above, the heat flux to soil was calculated on the basis of measurements below the natural underlying surface at the meteorological station located in a southern city precinct. Therefore, this dependence can be expected to have a larger amplitude under urban conditions, when materials making up the underlying surface have a much higher thermal conductivity coefficient. As a consequence, there will be much smaller differences between income and expense parts of the net thermal balance. It should be emphasized that February, 2005, had substantially different heat gain and loss. This period was characterized by sudden cooling with the formation of a well-pronounced temperature inversion. It can be hypothesized that cold advection in an anticyclone had been substantial in this case. This process is difficult to take into account in thermal balance studies because of complexities lying in measurements of heat fluxes in horizontal directions in the context of the monthly average.

CONCLUSIONS

Based on a complex study of all thermal balance components, we found that heat is mainly gained due to radiation components (75–100%) from March to September, and due to turbulent heat flux (from 40 to 85% of the total gain) from December to February. In the autumn period, prior to snow cover formation, the major contribution to the income part is made by the heat flux from soil, substantially increasing the turbulent heat flux to the atmosphere in this period of time.

The heat loss is partitioned between the turbulent heat flux and losses due to water evaporation (50/50%) in the warm period of the year. The heat loss to soil makes a fairly minor contribution (no more than 10% of total losses). In spring, the expense part is modified to include heat losses due to snow cover melting, which can reach 50% of the total loss in separate months. The heat losses are dominated by radiation components in winter.

The heat loss due to springtime snow cover melting is found to be substantial (30–50% of the total heat flux). At the same time, heat fluxes, released due to water freezing on the underlying surface in period of autumn frosts, as well as due to condensation of anthropogenic water vapor throughout the year, can be neglected.

It should be noted that, based on our study, large errors are characteristic for the most common method of thermal balance [2, 3], which, due to the lack of

data required to calculate the thermal balance components, they are then determined from equation (1).

ACKNOWLEDGMENTS

This work was supported by the Presidium of the Russian Academy of Sciences (Program no. 4); Department of Earth Sciences, Russian Academy of Sciences (Program no. 5); Siberian Branch, Russian Academy of Sciences (Interdisciplinary Integration Project nos. 35, 70, and 131), Russian Foundation for Basic Research (grant nos. 14-05-00526, 14-05-00590, and 14-05-93108); Ministry of Education and Science (State contract no. 14.604.21.0100, identification no. RFMTFIBBB210290; and State contract no. 14.613.21.0013; identification no. RFMEFI61314X0013).

REFERENCES

1. G. E. Landsberg, *Urban Climate* (Gidrometeoizdat, Leningrad, 1983) [in Russian].
2. M. I. Budyko, *Thermal Balance of the Earth's Surface* (Gidrometeoizdat, Leningrad, 1956) [in Russian].
3. A. M. Obukhov, *Turbulence and Atmospheric Dynamics* (Gidrometeoizdat, Leningrad, 1988) [in Russian].
4. L. S. Gandin, D. L. Laikhtman, L. T. Matveev, and M. I. Yudin, *Foundations of the Dynamic Meteorology* (Gidrometeoizdat, Leningrad, 1955) [in Russian].
5. M. I. Budyko, *Evaporation in Natural Conditions* (Gidrometeoizdat, Leningrad, 1948) [in Russian].
6. L. T. Matveev, *Atmospheric Physics* (Gidrometeoizdat, St. Petersburg, 2000) [in Russian].
7. M. Yu. Arshinov, B. D. Belan, D. K. Davydov, V. K. Kovalevskii, A. P. Plotnikov, E. V. Pokrovskii, T. K. Sklyadneva, and G. N. Tolmachev, "Automated station for atmospheric trace gas monitoring," Meteorol. Gidrol, No. 3, 110–118 (1999).
8. http://lop.iao.ru/activity/?id=tor
9. V. E. Zuev, B. D. Belan, D. M. Kabanov, V. K. Kovalevskii, O. Yu. Luk'yanov, V. E. Meleshkin, M. K. Mikushev, M. V. Panchenko, I. E. Penner, E. V. Pokrovskii, S. M. Sakerin, S. A. Terpugova, G. N. Tolmachev, A. G. Tumakov, V. S. Shamanaev, and A. I. Shcherbatov, "The "OPTIK-E" AN-30 aircraft-laboratory for ecological investigations," Atmos. Ocean. Opt. **5** (10), 658–663 (1992).
10. M. Yu. Arshinov, B. D. Belan, D. K. Davydov, G. A. Ivlev, A. S. Kozlov, V. S. Kozlov, M. V. Panchenko, I. E. Penner, D. A. Pestunov, A. S. Safatov, D. V. Simonenkov, G. N. Tolmachev, A. V. Fofonov, V. S. Shamanaev, and V. P. Shmargunov, "Aircraft laboratory Antonov-30 "Optik-E": 20-year investigations of the environment," Opt. Atmos. Okeana **22** (10), 950–957 (2009).
11. http://lop.iao.ru/activity/?id=fly
12. http://www.meteotomsk.ru/site
13. V. V. Antonovich, B. D. Belan, A. V. Kozlov, D. A. Pestunov, and A. V. Fofonov, "Separation of a contribution coming from city to variations of thermodynamic characteristics of the air in Tomsk as an example," Atmos. Ocean. Opt. **18** (8), 570–574 (2005).
14. http://lop.iao.ru/activity/?id=bec
15. http://tmsk.gks.ru/
16. http://tomsk.tgk11.com/
17. http://www.ensb.tomsk.ru/
18. http://www.gibdd.ru/r/70/contacts/div1169000/
19. N. V. Dudorova and B. D. Belan, "Radiation balance of the underlying surface in Tomsk in 2004–2005," Atmos. Ocean. Opt. **28**(4), 312–317 (2015).
20. B. D. Belan, O. A. Pelymskii, and N. V. Uzhegova, "Study of the anthropogenic component of urban heat balance," Atmos. Ocean. Opt. **22** (4), 441–446 (2009).
21. E. V. Shein, *Course of Soil Physics* (Mos. Gos. Univ., Moscow, 2005) [in Russian].
22. L. A. Bekhovykh, S. V. Makarychev, and I. V. Shorina, *Grounds for Hydrophysics* (AGAU, Barnaul, 2008) [in Russian].
23. A. F. Vadyunina and Z. A. Korchagina, *Methods for Investigating Physical Properties of Soils* (Agropromizdat, Moscow, 1986) [in Russian].
24. V. A. Gladkikh, A. E. Makienko, E. A. Miller, and S. L. Odintsov, "Study of the atmospheric boundary layer parameters under urban conditions with local and remote diagnostics facilities. Part 2. Air temperature and heat flux," Atmos. Ocean. Opt. **24** (3), 280–287 (2011).
25. *Instructions on Gradient Observations and Detection of Thermal Balance Components* (Gidrometeoizdat, Leningrad, 1964) [in Russian].
26. P. Brimblecombe, *Air Composition and Chemistry* (Cambridge University Press, Cambridge, 1986).
27. B. Offerle, C. S. B. Grimmond, and K. Fortuniak, "Heat storage and anthropogenic heat flux in relation to the energy balance of a central European city centre," Int. J. Climatol. **25** (10), 1405–1419 (2005).

Translated by O. Bazhenov